Gravity flow on steep slope: Part II

Christophe Ancey

23–24 June 2010

Outline

Today

- Fluid-mechanics approach to gravity flows
- Rheology
- Depth-averaged equations and lubrication theory
- Friction-dominated flows: use of asymptotic expansions
- Inertia-dominated flows: phase plane formalism
- Perspectives

Scales of investigation

Different scales and thus different classes of models

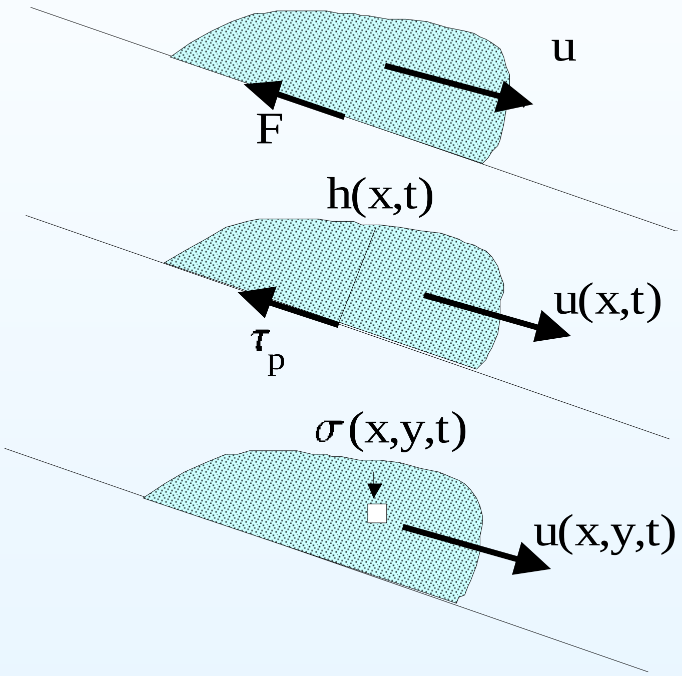

Flow regimes

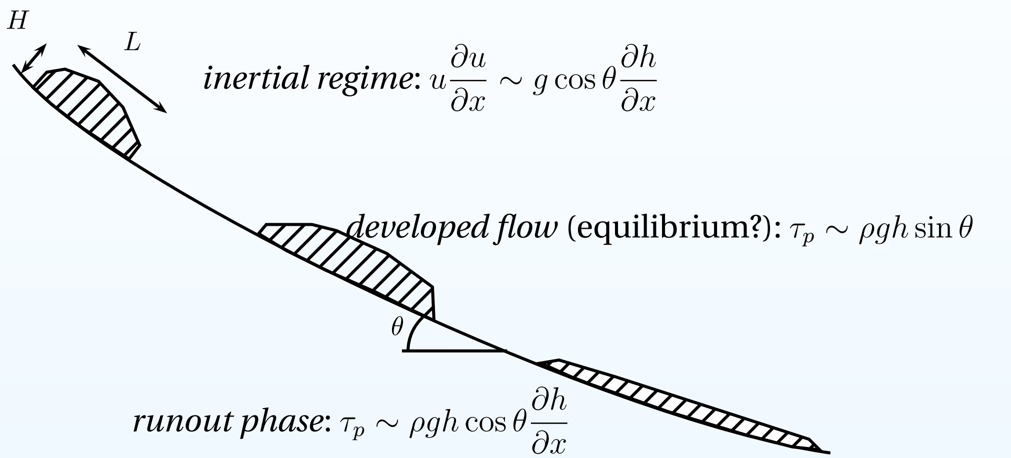

shallow-flow approximation: $$\frac{\partial u}{\partial t} + u\frac{\partial u}{\partial x} = g\sin\theta - g\cos\theta\frac{\partial h}{\partial x} - \frac{\tau_p}{\rho g h}$$

A usual working assumption: bulk dynamics are controlled by the body

- different regimes outlined using dominant-balance arguments
- influence of the front: boundary condition? Specific rheology and behavior?
- a few peculiarities: instabilities, entrainment (mass balance)

Avalanches in the laboratory: the dam-break problem

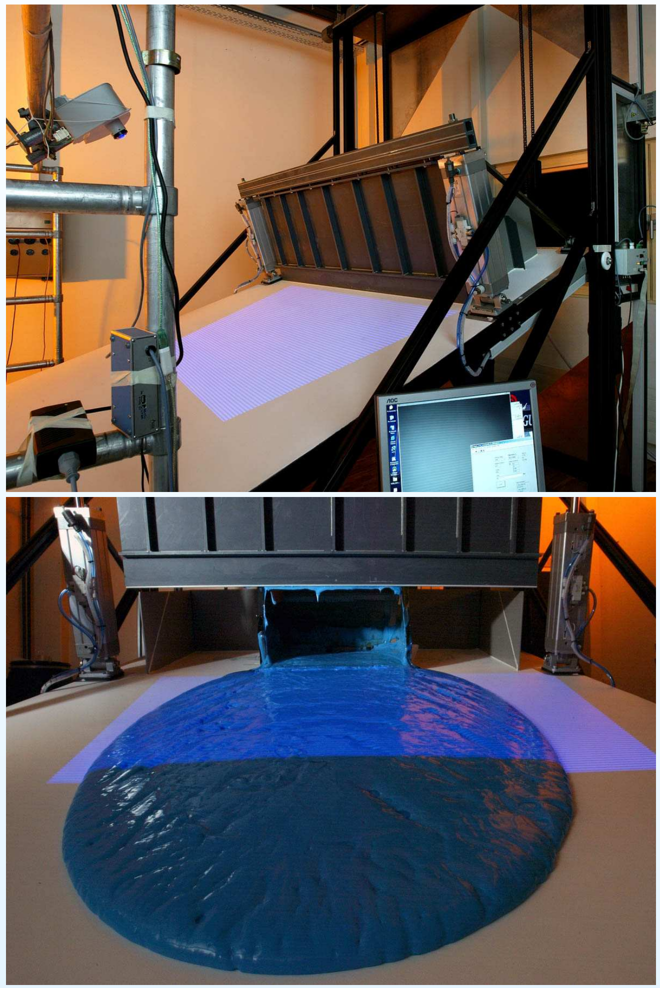

Experiments: Carbopol (polymeric gel) colored in blue.

Small-scale experiments: balance between pressure gradient, inertia, and viscous dissipation

- rheological behavior: imposed (and controlled rheometrically).
- initial and boundary conditions: known and controlled.

ÉCOLE POLYTECHNIQUE
FÉDÉRALE DE LAUSANNE

Measurement system: 3D surface reconstruction

Flow visualization

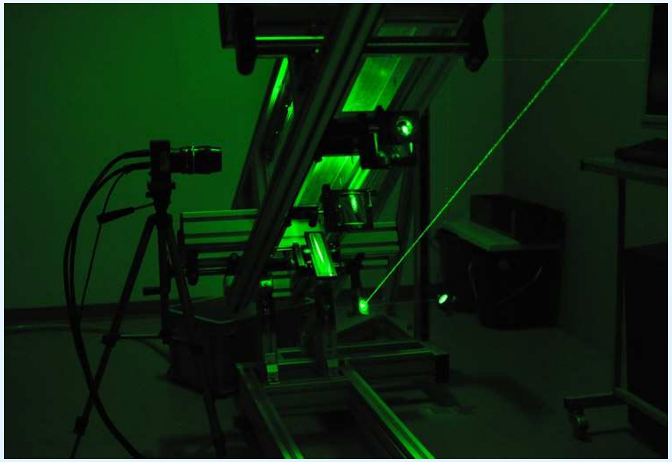

Snow rheology

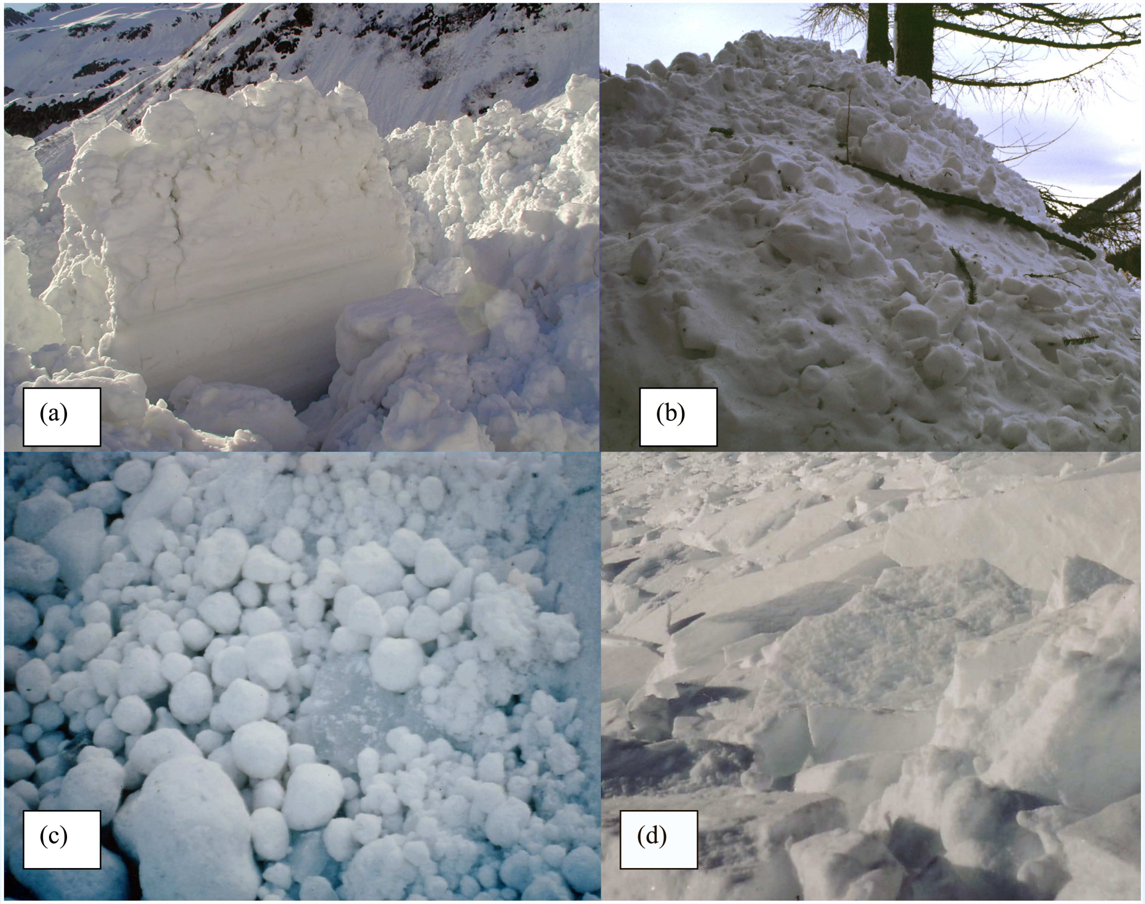

Influence on flow dynamics

Trajectory and deposit depending snow features

Courtesy Office fédéral de la topographie. Geschinen (VS) 23 Feb. 1999.

Inference from field data

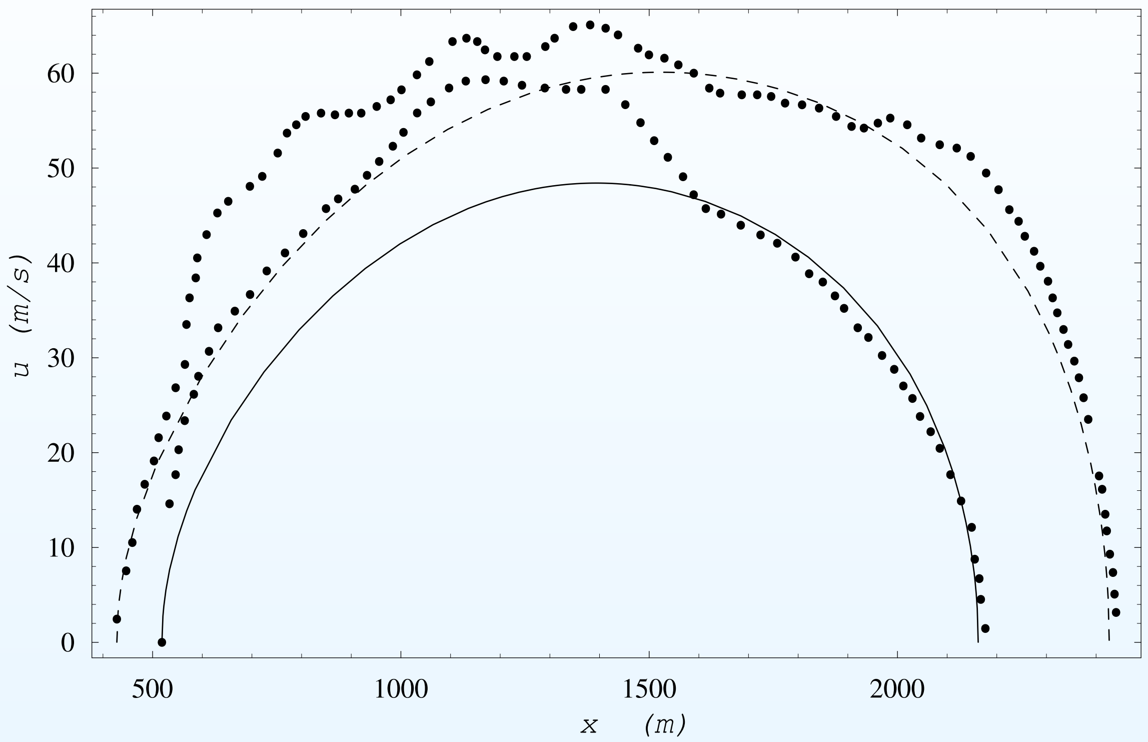

Coulomb model: $F_x = \mu m g \cos\theta$, μ adjusted from x_{stop}

Sliding-block approximation

Governing equation for a sliding block

$$m\frac{d\mathbf{u}}{dt} = m\mathbf{g} + \mathbf{F}(\mathbf{u})$$

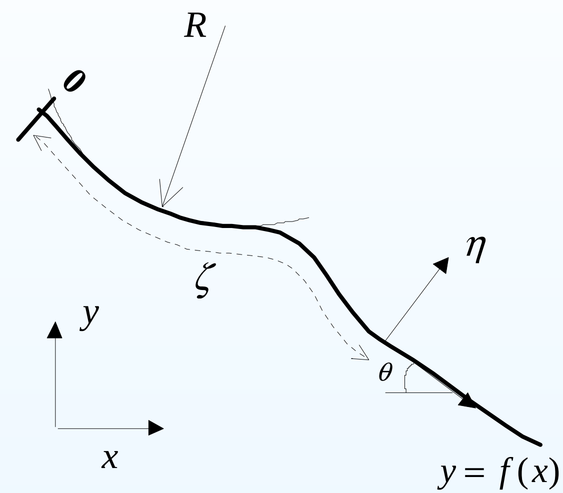

Projection onto the path

$$\frac{F_\zeta}{m} = g\sin\theta(\zeta) - u\frac{du}{d\zeta} + \text{curvilinear terms}$$

Knowing the velocity variations and the path profile makes it possible to deduce the bulk frictional force.

Frictional behavior

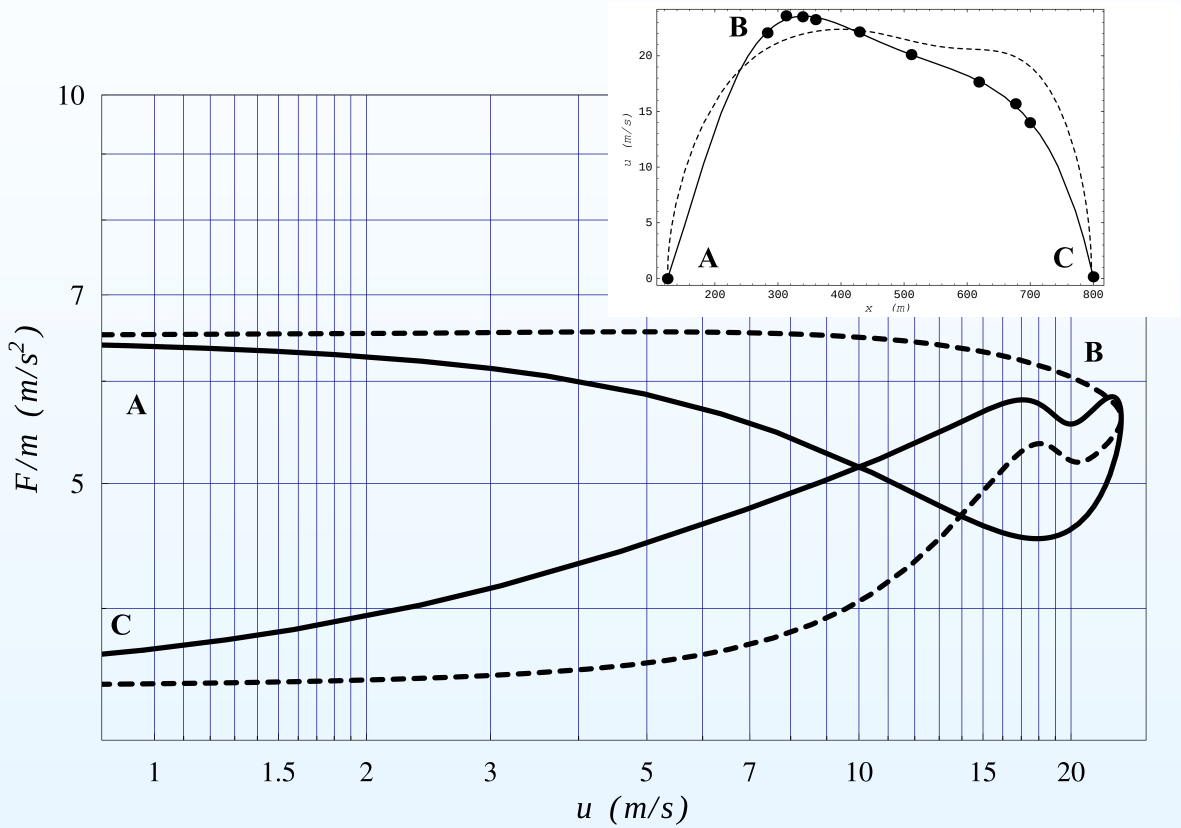

ÉCOLE POLYTECHNIQUE
FÉDÉRALE DE LAUSANNE

Velocity-dependent behavior

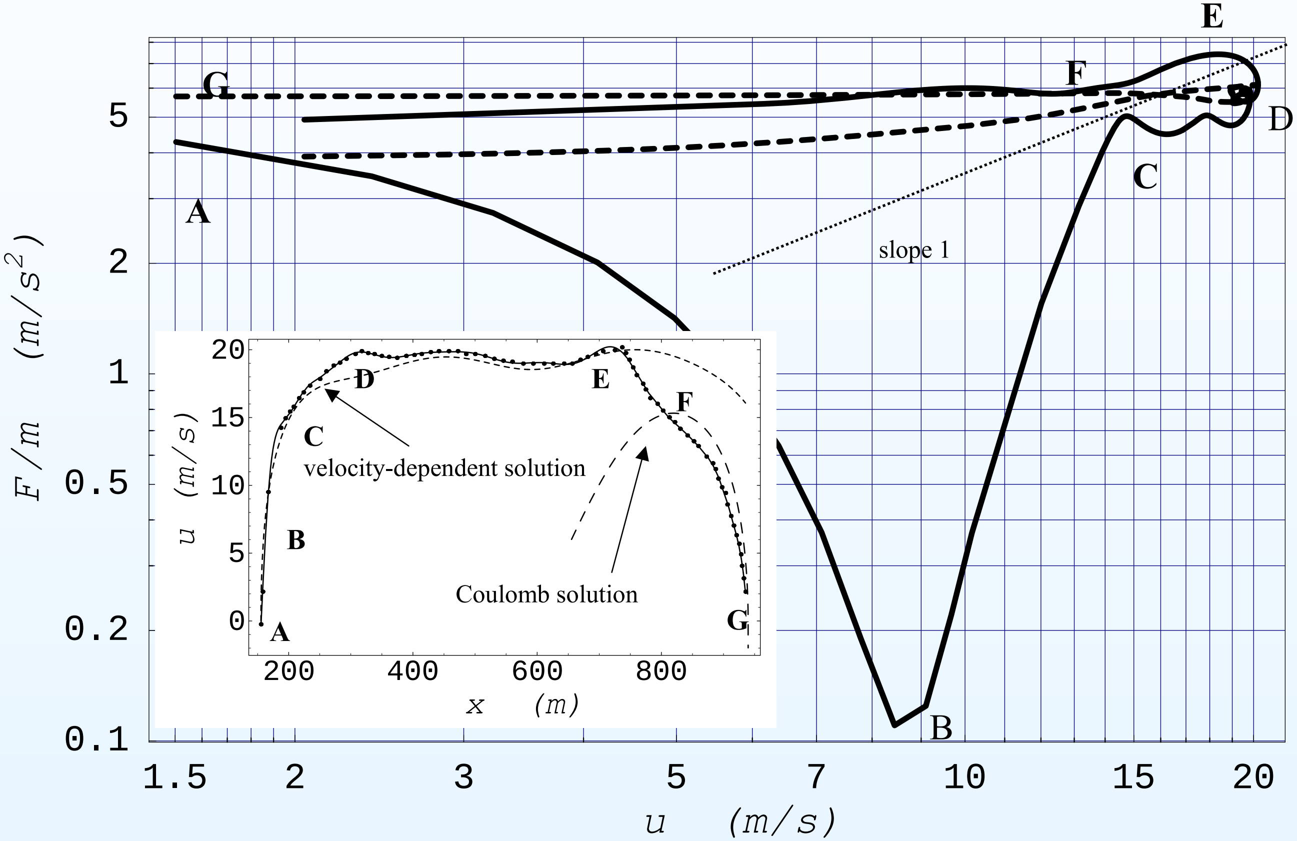

Mud rheometry

Experimental investigations conducted on natural materials or nearly natural materials providing evidence of viscoplastic behavior.

Authors	Experiments
O'Brien & Julien (1988)	viscometric tests on natural mudflow deposits
Coussot (1997), Coussot & Piau (1995), Coussot *et al.* (2003)	Couette rheometer on fine mud samples
Coussot *et al.* (1998)	wide-gap Couette rheometer with debris-flow samples
Bardou *et al.* (2003)	Couette rheometer and special rheometers used for concrete on debris-flow samples
Remaître et al. (2005)	Couette rheometer on fine mud samples
Major & Pierson (1992)	Couette rheometer with fine-grained materials collected on debris-flow deposits
Martino (2003)	Couette rheometer with natural samples
Schatzmann *et al.* (2003)	special BMS rheometer with natural samples
Parsons *et al.* (2001)	flume with artificial mixtures made up of clay, silt, and sand
Sosio & Crosta (2009)	Couette rheometer on sand and clay samples

Viscoplastic model

Herschel-Bulkley model

$$\tau = \tau_c + K\dot{\gamma}^n, \quad (1)$$

with τ_c the yield stress, K and n two constitutive parameters, all dependent on solid concentration.

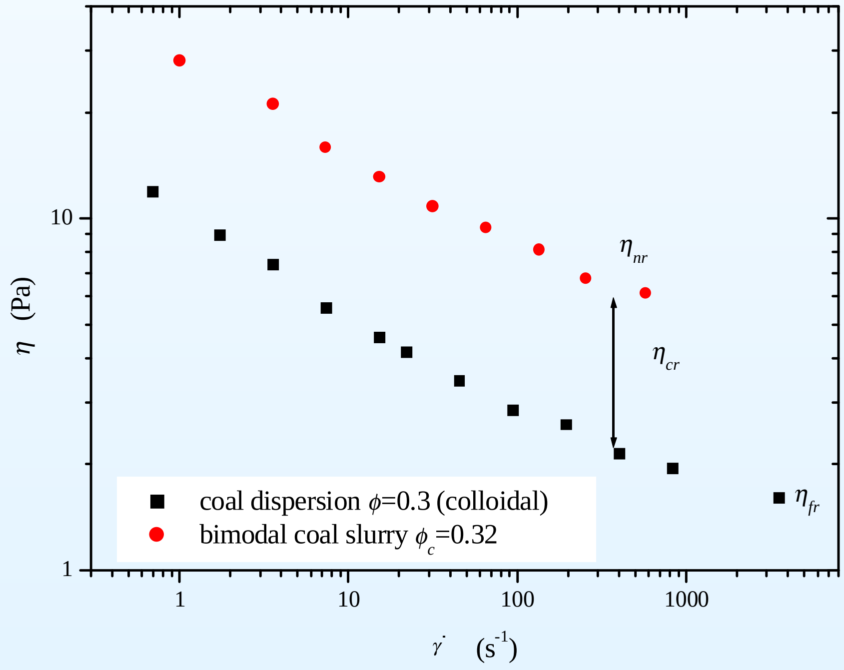

Variation in the bulk viscosity η of coal slurry as a function of the shear rate. The bulk viscosity curve is parallel to the curve obtained with the fine fraction.

Effect of solid concentration

Variation in the bulk yield stress

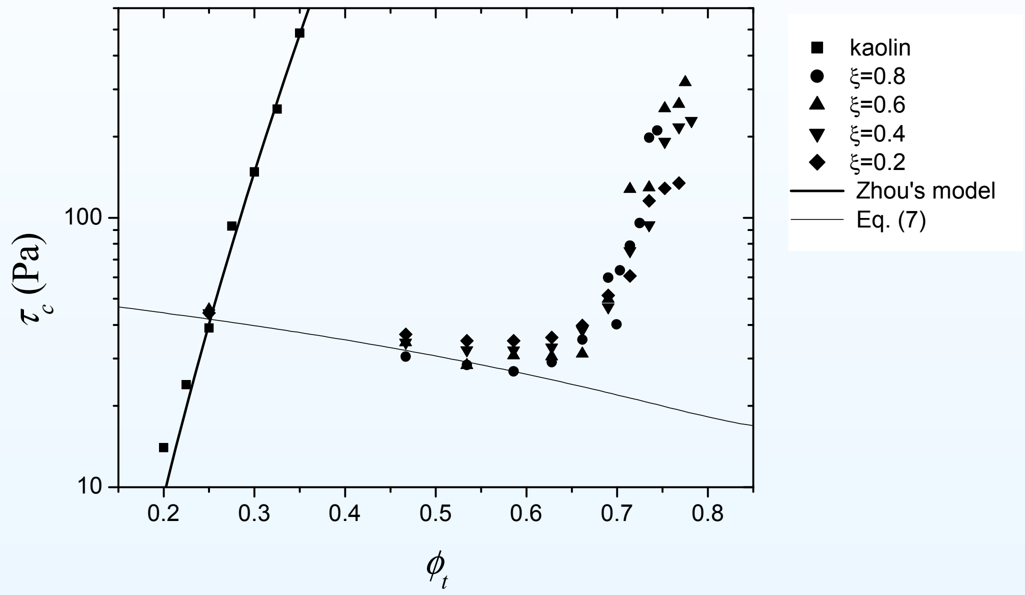

- Adding a small amount of coarse particles leads to a decrease in the bulk yield stress.
- Interestingly enough, the bulk yield stress starts diverging when the total solid concentration comes closer to the maximum solid concentration.
- A striking feature of this abrupt rise is that the increase rate is very close to the value measured for a pure kaolin dispersion.

Empirical constitutive equations

Coulomb law (Iverson's model)

$$\tau = \sigma' \tan\varphi, \tag{2}$$

with $\sigma' = \sigma - p$ (with p the interstitial pore pressure).

Frictional-collisional model (Savage)

$$\tau = \sigma \tan\varphi + \mu(T)\dot{\gamma}, \tag{3}$$

with T the granular temperature.

Coulomb-number dependent relation

$$\tau = \sigma \tan\varphi + \mu(\mathrm{Co})\dot{\gamma}. \tag{4}$$

with the Coulomb number $\mathrm{Co} = \rho_p a^2 \dot{\gamma}^2 / \sigma$.

Empirical constitutive equations (2)

Alternative representations (Pouliquen *et al.*)

$$\tau = \sigma \, \tan \varphi(\mathrm{I}). \tag{5}$$

with $I = \mathrm{Co}^{-1/2}$ the inertial number. Josserand's relation is based on the solid concentration ϕ

$$\tau = K(\phi)\sigma + \mu(\phi)\dot{\gamma}^2, \tag{6}$$

Governing equations: a shallow world

Most models used for computing the behavior of an avalanching mass are based on the shallow-flow approximation: $\epsilon = H/L \ll 1$.

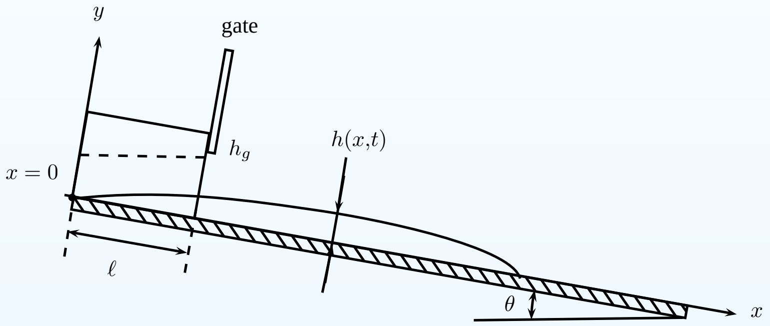

There are two approaches

- Flow-depth averaged equations: historical approach used by Saint-Venant (floods), Savage & Hutter (granular flows), Iverson & Denlinger, Mangeney & Bouchut and many others...
- Lubrication approximation: pioneering work conducted by Reynolds and subsequent authors (boundary layer theory), renewed interest with the work done by Mei & Liu, Huppert, Balmforth & Craster.

Shallow-flow equations

A versatile set of equations

$$\frac{\partial h}{\partial t} + \frac{\partial h\bar{u}}{\partial x} = E - D,$$

$$\frac{\partial h\bar{u}}{\partial t} + \beta \frac{\partial h\bar{u}^2}{\partial x} = \rho g h - k g h \frac{\partial h}{\partial x} - \frac{\tau_b}{\rho},$$

with β Boussinesq coefficient (usually set to unity), k a pressure coefficient, and τ_b the bottom shear stress, E and D entrainment and deposition rates.

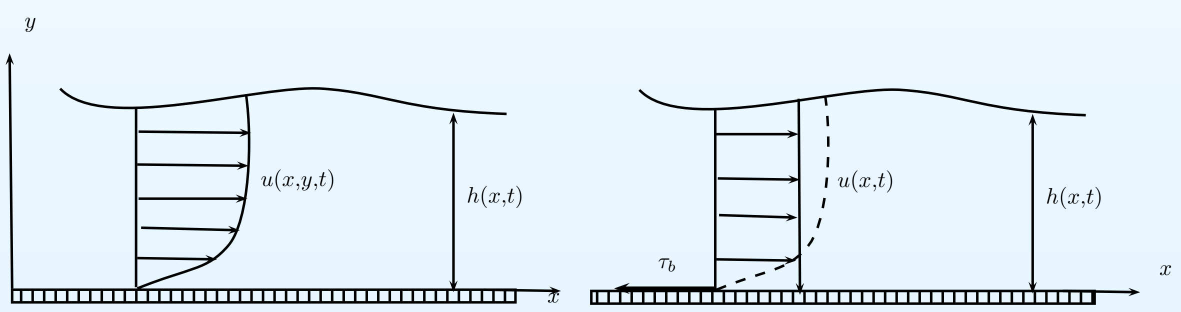

Information is averaged when deriving the governing equations, which makes it difficult to properly define the coefficients that come up in the final equations.

ÉCOLE POLYTECHNIQUE
FÉDÉRALE DE LAUSANNE

Strength and weakness

The shallow-water equations offer a reasonably accurate physical framework for describing a host of natural phenomena. The governing equations are now well “tamed” by numerical methods. Numerical schemes for 1D and 2D models are reasonably fast and make it possible to simulate complex flows (e.g., tsunamis) on large scales. However, when dealing with geophysical flows on steep slopes, we are faced with many issues:

- tracking the front position;
- computing the internal dissipation and account for it through τ_p;
- taking additional terms induced by irregular topography into account;
- evaluating mass balance and its effect on the bulk dynamics;
- estimating the change in the bulk composition (e.g., segregation) and local rheology.

Lubrication approximation

Starting with the Cauchy equations (mass and momentum balance equations), we scale the variables

$$\tilde{u} = u/U_*,\ \tilde{x} = x/L_*,\ \tilde{y} = y/(\epsilon L_*),\ \tilde{p} = p/P_*,\ \tilde{p} = p/P_*, \ldots$$

with $\epsilon = H_*/L_*$ and make a power ϵ-expansion of the scaled variables: $\tilde{u} = \tilde{u}_0 + \epsilon \tilde{u}_1 + \ldots$. Collecting together the terms associating the same power of ϵ, we end up with a hierarchy of equations. For instance, we have

$$\epsilon \mathrm{Re} \frac{\mathrm{d}u}{\mathrm{d}t} = 1 - \epsilon \cot\theta \frac{\partial p}{\partial x} + \epsilon^{n+1} \frac{\partial \sigma_{xx}}{\partial x} + \frac{\partial \sigma_{xy}}{\partial y}, \quad (7)$$

$$\epsilon^2 \mathrm{Re} \frac{\mathrm{d}v}{\mathrm{d}t} = -\cot\theta \left(1 + \frac{\partial p}{\partial y}\right) + \epsilon \frac{\partial \sigma_{xy}}{\partial x} + \epsilon^n \frac{\partial \sigma_{yy}}{\partial y}, \quad (8)$$

ÉCOLE POLYTECHNIQUE
FÉDÉRALE DE LAUSANNE

Lubrication approximation (continued)

To order ϵ^0, we have to solve

$$0 = 1 + \frac{\partial \sigma_{0,xy}}{\partial y}, \quad (9)$$

$$0 = -1 - \frac{\partial p_0}{\partial y}, \quad (10)$$

a much simpler set of equations than the full governing equations! In the limit of $\mathrm{Re} \to 0$ and to order ϵ, we obtain

$$0 = -\cot\theta \frac{\partial p_0}{\partial x} + \frac{\partial \sigma_{1,xy}}{\partial y}, \quad (11)$$

$$0 = -\cot\theta \frac{\partial p_1}{\partial y} + \frac{\partial \sigma_{0,xy}}{\partial x}, \quad (12)$$

Application to Newtonian avalanches

To leading order, the governing equation for h writes

$$\frac{\partial h}{\partial t} + \underbrace{\frac{\partial h^3}{\partial x}}_{convection} = \underbrace{\frac{\partial}{\partial x}\left(h^3\frac{\partial h}{\partial x}\right)}_{diffusion}. \tag{13}$$

Analytical solutions can be worked out in terms of similarity solutions at late and early times:

$$h(x,t) = t^{-n}H(\xi,t)$$

with $\xi = x/t^n$.
Substituting into (13) gives $n = 1/3$ (late time solution) or $n = 1/5$ (early time solution). Depending on the initial conditions, convergence towards the similarity solution can be slow.

Application to Newtonian avalanches (continued)

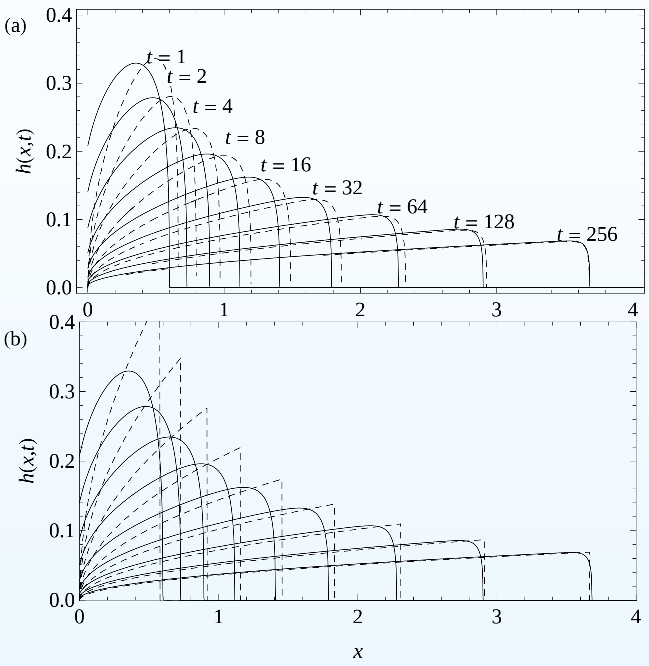

Flow-depth profiles provided by numerical solutions (solid line) of the nonlinear diffusion equation for $\theta = 6^\circ$ at dimensionless times $t = 1$, 2, 4, 8, 16, 32, 64, 128, and 256. In subplot (a), we plotted the analytical approximation obtained by composing the inner and outer similarity solutions (dashed line). In subplot (b), the analytical solution corresponding to pure convection is reported.

Convective regime

At long times, we end up with a nonlinear convection equation:

$$\frac{\partial h}{\partial t} + \frac{\partial h^3}{\partial x} = 0, \tag{14}$$

which can be recast into the characteristic form

$$\frac{\mathrm{d}h}{\mathrm{d}\tau} = 0 \text{ along } \frac{\partial t}{\partial \tau} = 1 \text{ and } \frac{\partial x}{\partial \tau} = 3h^2, \tag{15}$$

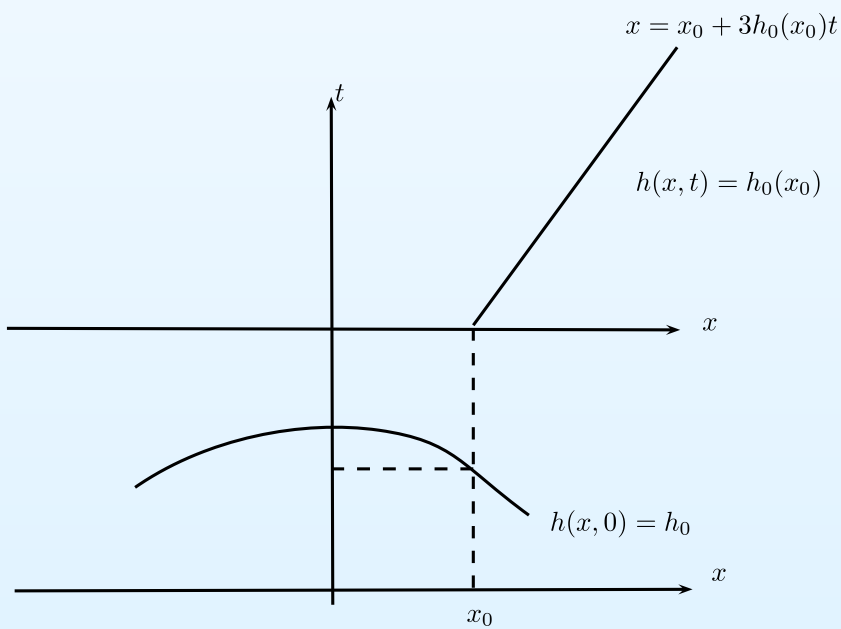

Front behavior

Singularity at the front (boundary layer). We make the following change of variable

$$x' = \frac{x - x_f(t)}{\epsilon}.$$

In the mobile frame attached to the front, the dominant balance in the momentum balance equation is between the streamwise gradient of the pressure and the cross-stream gradient of the shear stress. Since $h = O(\epsilon)$ and $\cot\theta\epsilon^{1/2} = O(1)$, we then pose

$$\epsilon = \tan^2\theta.$$

We now embody this scaling analysis into an asymptotic analysis by substituting the following stretched variables into the governing equations: $x = x_f + \epsilon x'$, $y = \epsilon y'$, $t = \epsilon t'$,
$u = \epsilon^{3/2} u' = \epsilon^{3/2} u'_0 + \cdots$, $v = \epsilon^{3/2} v' = \epsilon^{3/2} v'_0 + \cdots$,
$h = \epsilon h'_0 + \cdots$, and $p = \epsilon p'_0 + \cdots$.

Matched asymptotic expansions

The re-scaled momentum balance equations are

$$\epsilon^{1/2}\mathrm{Re}\left(\frac{\mathrm{d}u}{\mathrm{d}t'} - \dot{x}_f\frac{\partial u}{\partial x'}\right) = 3\epsilon^{1/2} - 3S\frac{\partial p}{\partial x'} + \epsilon^2\frac{\partial^2 u'}{\partial x'^2} + \frac{\partial^2 u'}{\partial y'^2}, \quad (16)$$

$$\epsilon^{3/2}\mathrm{Re}\left(\frac{\mathrm{d}v}{\mathrm{d}t'} - \dot{x}_f\frac{\partial v}{\partial x'}\right) = -3\cot\theta\left(1 + \frac{\partial p}{\partial y}\right) + \epsilon^{5/2}\frac{\partial^2 v'}{\partial x'^2} + \epsilon^{1/2}\frac{\partial^2 v'}{\partial y'^2}. \quad (17)$$

The evolution equation for the flow depth is then

$$\frac{\partial h}{\partial t'} + \frac{\partial}{\partial x'}G(h) = 0, \text{ with } G(h) = -h^3\cot\theta\frac{\partial h}{\partial x'}$$

That is a nonlinear diffusion that can be solved numerically (e.g. using the built-in function *pdepe* in Matlab); exact similarity solution also exist (providing the long-term behavior).

Comparison with data

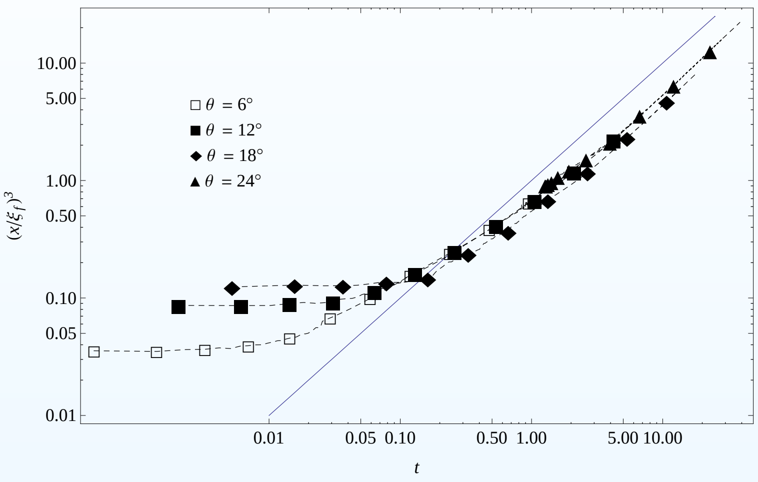

Normalized front position $(x_f/\xi_f)^3$ as a function of time in a log-log representation: the experimental curves (dashed line marked with symbols) related to $\theta = 6^\circ$, 12°, 18°, and 24° slopes are indicated. The solid line represents the theoretical curve $(x/\xi_f)^3 = t$ corresponding to the outer similarity solution.
Fluid: glycerol $\mu \sim 345$ Pa.s (molten toffee)

Comparison with data (2)

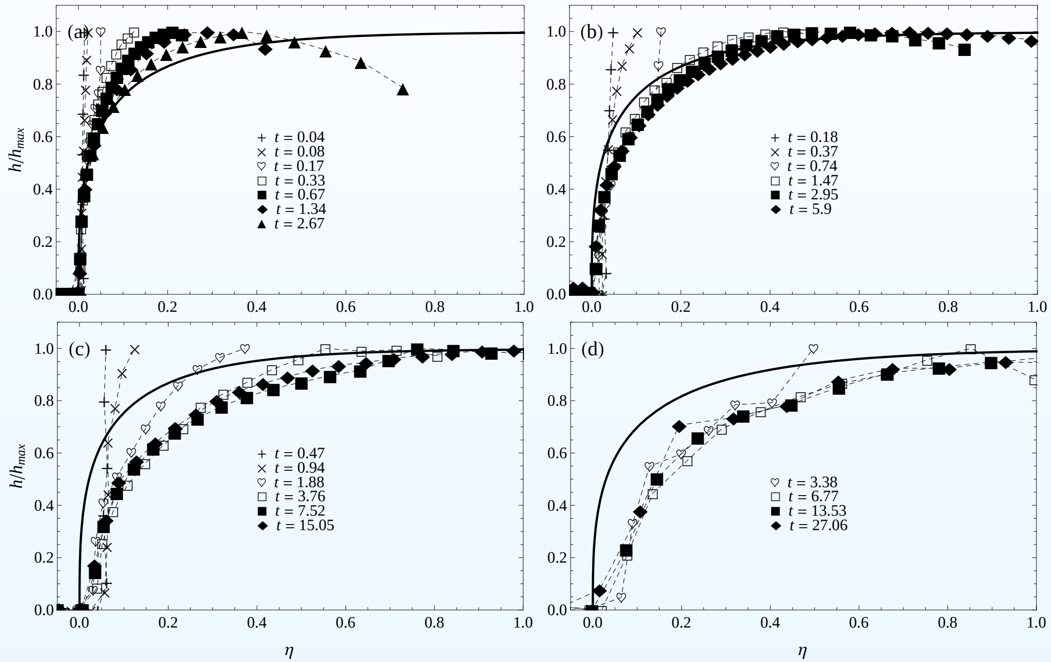

Flow-depth profiles $h(\eta, t)$ normalized by the maximum flow depth h_{max} for $\theta = 6^\circ$ (a), $\theta = 12^\circ$ (b), $\theta = 18^\circ$ (c), and $\theta = 24^\circ$ (d) at different dimensionless times. We also plotted the composite solutions (thick line).

ÉCOLE POLYTECHNIQUE
FÉDÉRALE DE LAUSANNE

Application to viscoplastic avalanches

The same techniques can be applied to viscoplastic materials.

$$\frac{\partial h}{\partial t} + \frac{\partial}{\partial x} F(h) = 0,$$

with $Y = \max\left(h - Bi, 0\right)$ and

$$F(h) = nY^{1+1/n} \frac{(2n+1)h - nY}{(2n+1)(n+1)} \text{ and } Bi = \frac{\tau_c}{K\left(\frac{U_*}{H_*}\right)^n}.$$

Comparison with data

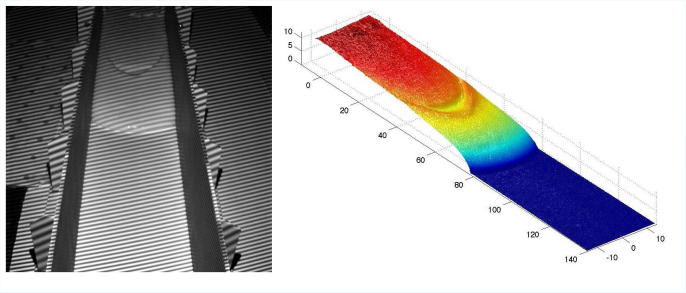

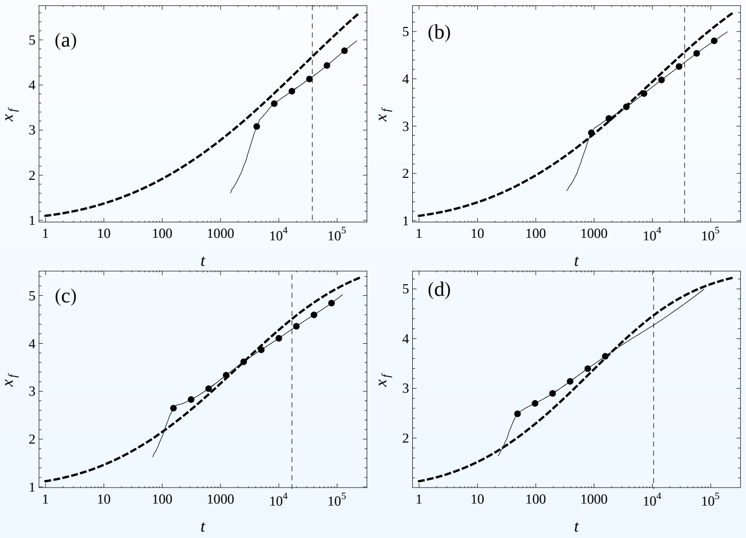

Variation in the front position with time for $\theta = 24^\circ$. Experiments done with Carbopol at various concentrations. Dashed curves: theoretical prediction given by a zero-order nonlinear convection equation (modelling the behavior of an avalanching mass of Herschel-Bulkley fluid).

Comparison with data (continued)

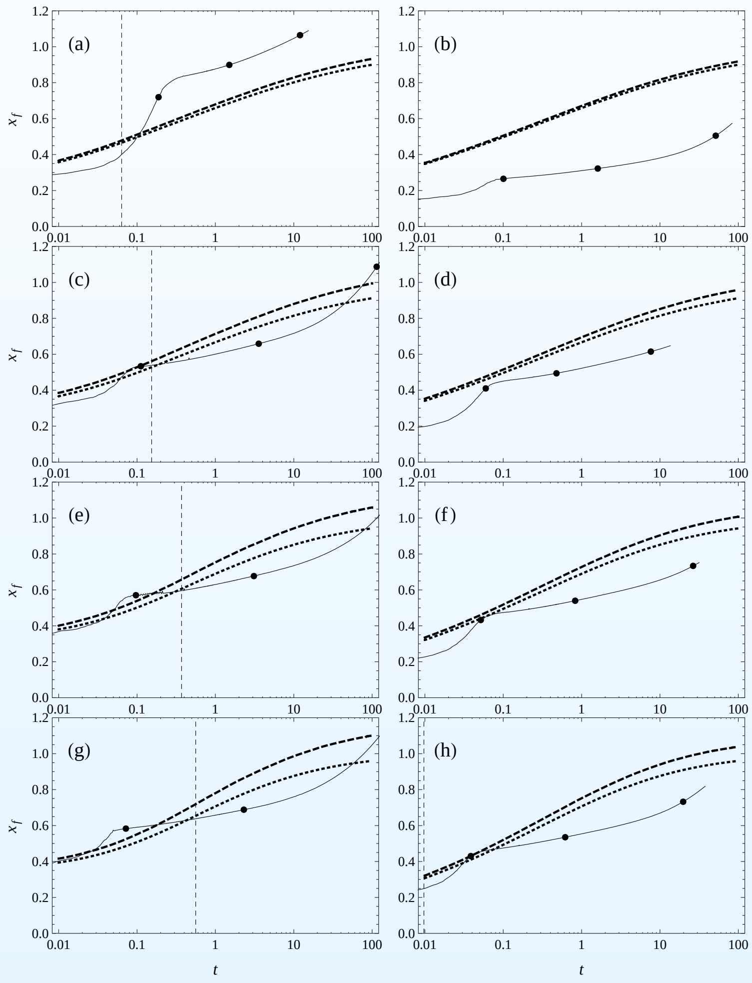

Variation in the front position with time for $\theta = 12^\circ$. Experiments done with Carbopol at various concentrations. Dashed curves: theoretical prediction given by a zero-order nonlinear convection equation (modelling the behavior of an avalanching mass of Herschel-Bulkley fluid).

ÉCOLE POLYTECHNIQUE
FÉDÉRALE DE LAUSANNE

Problem to solve

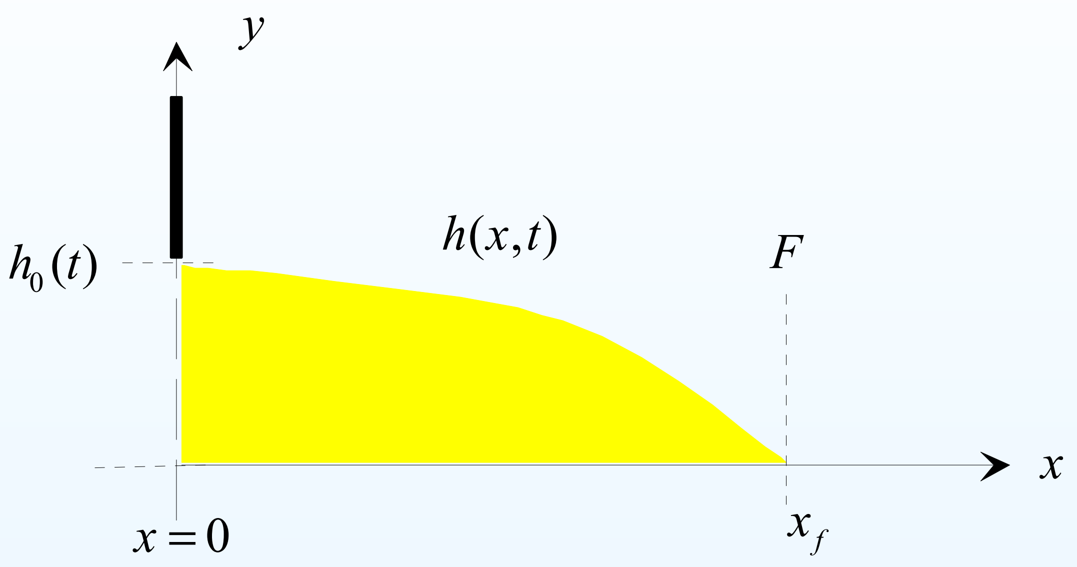

- flow on horizontal bottom
- no entrainment (density constant)
- friction negligible (inertial regime), no Benjamin boundary condition at the Front
- shear in the upward direction $\overline{u^2} = \gamma \bar{u}^2$ with $\gamma \neq 1$
- released volume: $\mathcal{V} = \int_0^{x_f} h(x,\ t)dx = At^n$.

Goals:

- compute $x_f(t)$

ÉCOLE POLYTECHNIQUE
FÉDÉRALE DE LAUSANNE

Shallow-water equations

$$\frac{\partial h}{\partial t} + \frac{\partial h\bar{u}}{\partial x} = 0,$$

$$\frac{\partial \bar{u}}{\partial t} + (2\gamma - 1)\bar{u}\frac{\partial \bar{u}}{\partial x} + \bar{u}^2\frac{\partial \gamma}{\partial x} = -\frac{\partial h}{\partial x}\left(1 + \frac{\bar{u}^2}{h}(\gamma - 1)\right).$$

Similarity forms

$u = \delta\xi t^{\delta-1}V(\xi)$, $h = \delta^2\xi^2t^{2(\delta-1)}Z(\xi)$, and $\xi = \frac{x}{t^\delta}$,

Boundary conditions

- At the front $Z(\xi_f) = 0$ and $V(\xi_f) = 1$ (non-Boussinesq regime).
- At the front $Z(\xi_f) = Fr_f^2$ and $V(\xi_f) = 1$ (Boussinesq regime: Benjamin condition).
- At the entrance:

$$Z \propto \beta\frac{1}{\delta^2\xi^2} \text{ and } V \propto \beta^{3/2}\alpha\frac{1}{\delta\xi} \text{ when } \xi \to 0.$$

Matrix form

$$\mathbf{M}(V,\ Z)\frac{d\mathbf{w}}{d\xi} = \frac{Z}{\delta\xi}\mathbf{S}(V,\ Z),$$

with $\mathbf{w} = [Z,\ V]^{\mathrm{T}}$,

$$\mathbf{M} = \begin{bmatrix} V-1 & Z \\ (\gamma-1)V^2 + Z & Z(V(2\gamma-1)-1) \end{bmatrix},\ \text{and}$$

$$\mathbf{S} = \begin{bmatrix} 3V\delta - 2 \\ 2\delta Z + V(V(4\gamma-3)\delta - 1) \end{bmatrix}.$$

The determinant of the matrix $\mathbf{M}$ is $\det\mathbf{M} = \delta Z\left(Z - I(V)\right)$, with $I(V) = 1 + (V-2)V\gamma$.

Phase-plane formalism

Regular and critical points ($F = 0$ and $G = 0$)

$$\frac{\mathrm{d}Z}{\mathrm{d}V} = \frac{F(V,\, Z)}{G(V,\, Z)}.$$

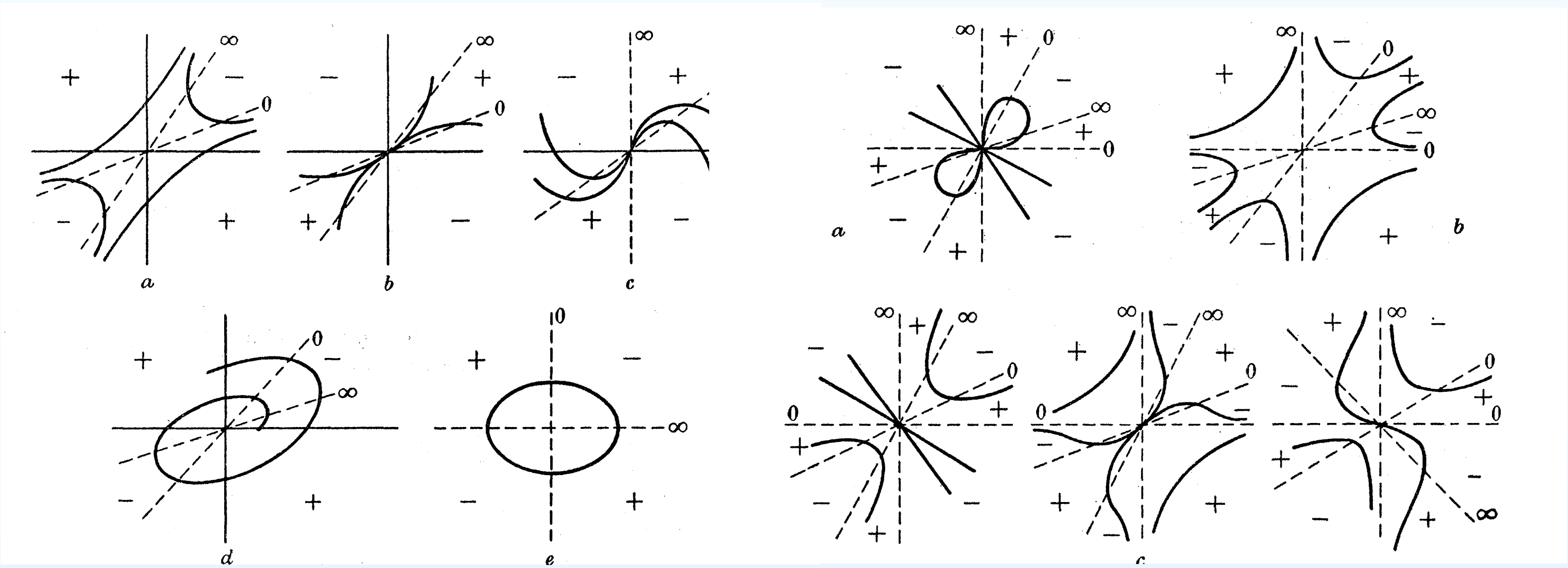

Phase-plane for $\gamma > 1$

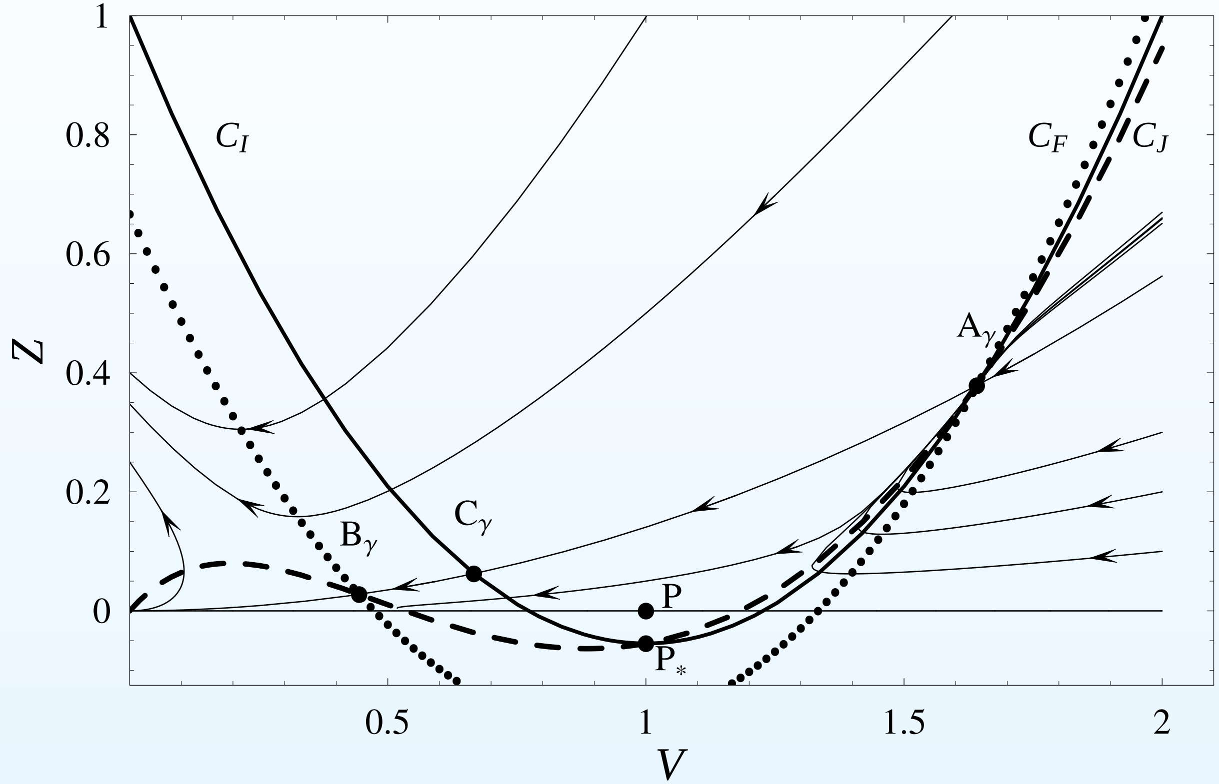

Problem: how to join S (source) and P (front point)?

Phase-plane for $\gamma = 1$

For $\gamma = 1$ the symmetry curve of the critical point (node) A passes through P

$$\frac{\mathrm{d}Z}{\mathrm{d}V} = \frac{F(V,\ Z)}{G(V,\ Z)}$$

$$Z' = \frac{V_A F_V + Z_A F_Z + \cdots}{V_A G_V + Z_A G_Z + \cdots}$$

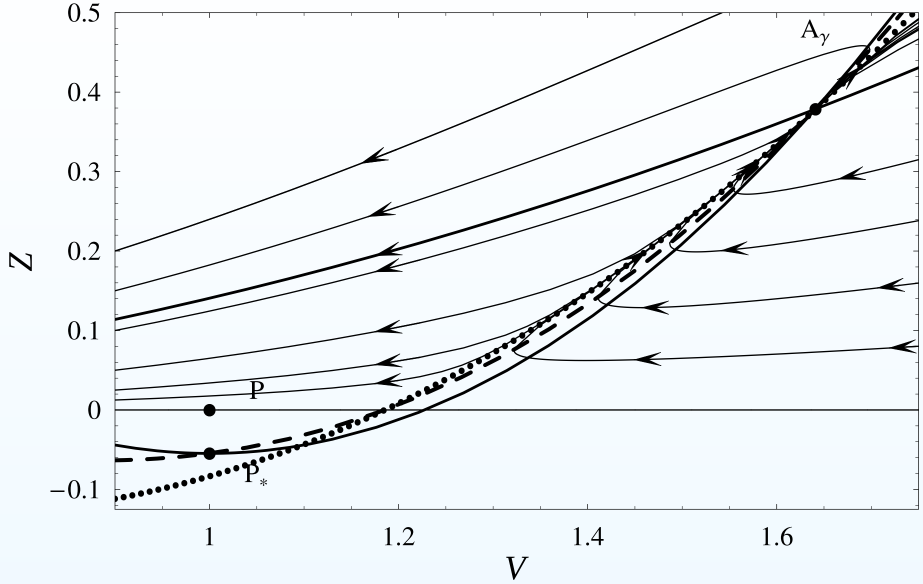

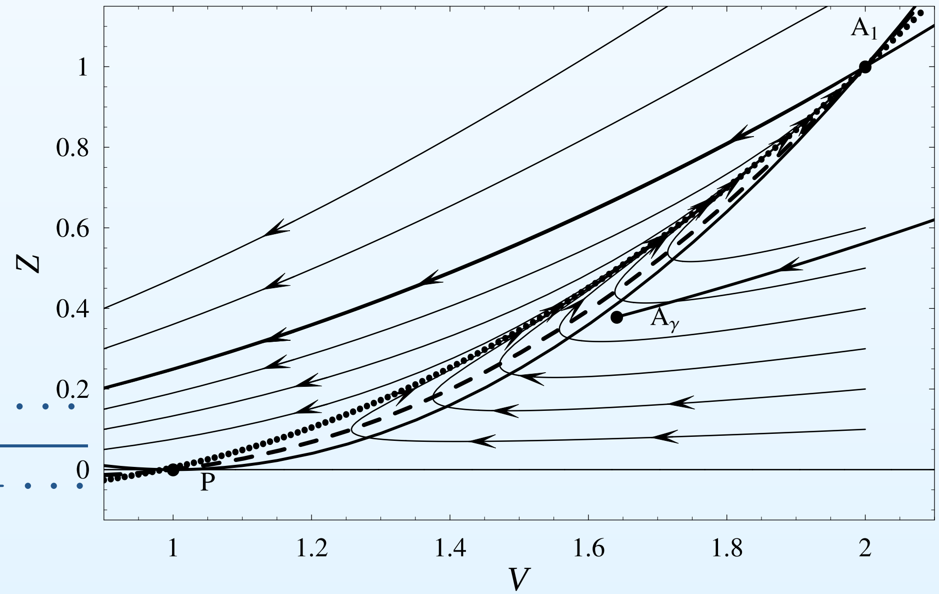

Solution for for $\gamma > 1$

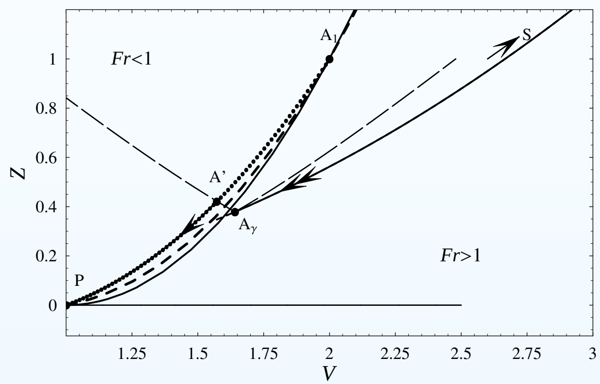

Jump between A_γ and A'

Dashed line: approximate (i.e., to first order) analytical solution to the Euler equations

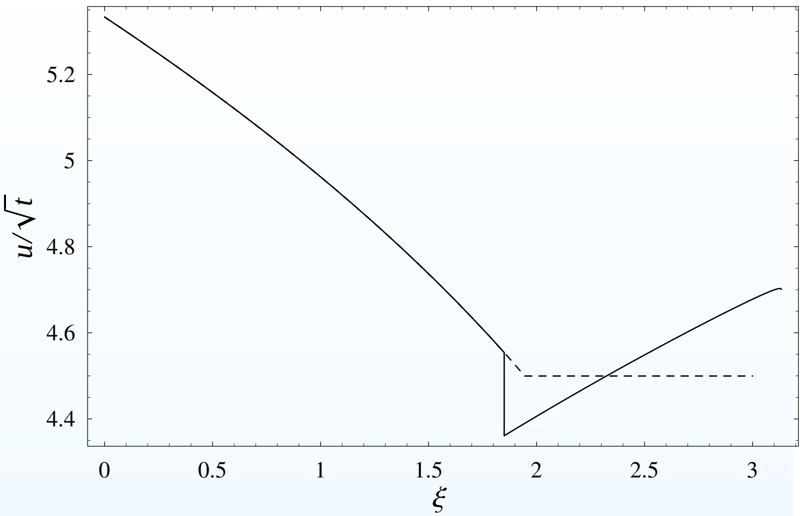

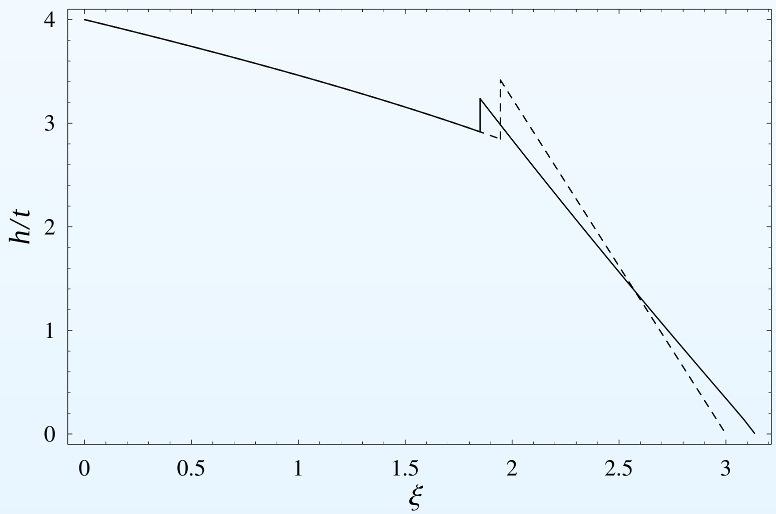

Conclusions

- A more physical construction of the solution in the tip region
- For non-Boussinesq regimes, subcritical similarity solutions does not exist.
- Supercritical similarity solutions exist for a limited range of volume growth n

$$V = \int_0^{x_f} h(x,\, t)\mathrm{d}x = At^n,$$

with $1 \leq n < 2$.

Ongoing and future research

- mass balance: how material is incorporated and deposited?
- shallow flows: do the flow-depth-averaged equations perform well when used to modelling unsteady fixed-volume surges?
- flow structure: particle flows, segregation, two-phase aspects, etc.
- stochastic modelling: coupling deterministic and stochastic models (MCMC models).

Segregation

Segregation and diffusive remixing can be modelled by a nonlinear advection diffusion equation

$$\frac{\partial \phi_s}{\partial t} + \text{div}(\phi_s \mathbf{u}) - \frac{\partial}{\partial z}\Big(q\phi_s(1-\phi_s)\Big) = \frac{\partial}{\partial z}\left(D\frac{\partial \phi_s}{\partial z}\right). \quad (18)$$

[Gray *et al.*, JFM]

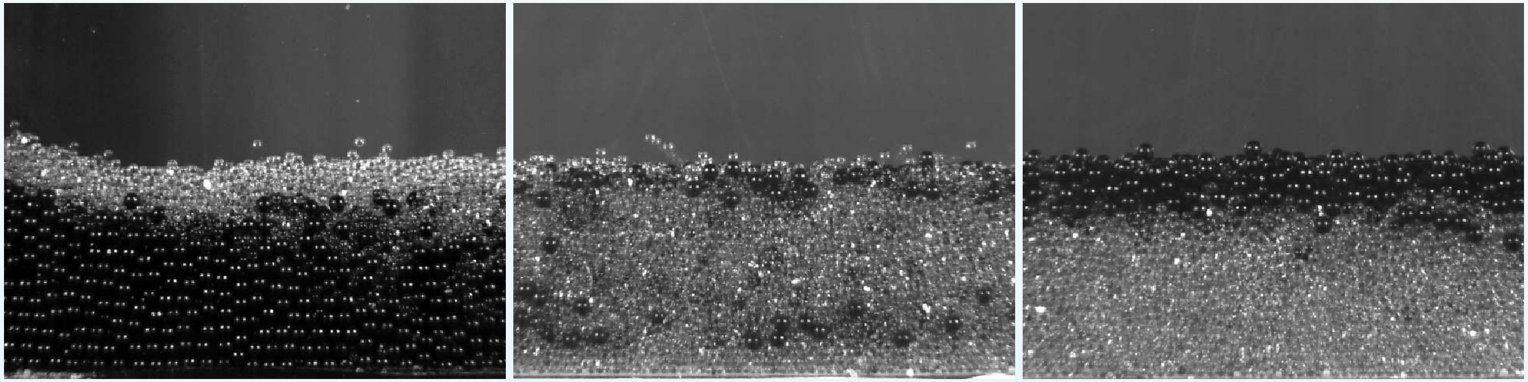

ÉCOLE POLYTECHNIQUE
FÉDÉRALE DE LAUSANNE

Comparison with data